Optimal Aperture Distribution for Maximum Power Transfer in Planar Lossy Multilayered Matters

9th European Conference on Antennas and Propagation, EuCAP 2015, Lisbon, Portugal, 13-17 May 2015

Citation for the published paper:
Razavi, A. ; Maaskant, R. ; Sipus, Z. et al. (2015) "Optimal Aperture Distribution for Maximum Power Transfer in Planar Lossy Multilayered Matters". 9th European Conference on Antennas and Propagation, EuCAP 2015, Lisbon, Portugal, 13-17 May 2015

(article starts on next page)

Optimal Aperture Distribution for Maximum Power Transfer in Planar Lossy Multilayered Matters

A. Razavi*, R. Maaskant*, J. Yang*, Z. Šipuš†, and M. Viberg*

*Dept. Signals and Systems, Chalmers University of Technology, Gothenburg, Sweden.
aidin.razavi@chalmers.se, rob.maaskant@chalmers.se, jian.yang@chalmers.se, mats.viberg@chalmers.se
†Faculty of Electrical Engineering and Computing, University of Zagreb, Zagreb, Croatia, zvonimir.sipus@fer.hr

***Abstract*—We combine array-signal-processing and spectral domain techniques to determine the optimal aperture current distribution that maximizes the power coupling between two antenna apertures which are located on opposing sides of a multilayered lossy structure in the near-field. The resulting optimal distribution can be used as a reference in the design of antennas for near-field applications, such as for the detection of foreign objects in lossy media, wireless charging of implant batteries, or near-field communications with an implant. A MoM approach is formulated to study the performance of the optimal aperture currents in a simulated detection application in the presence of a small PEC patch, and it is shown that the optimal aperture current can improve the system sensitivity and increase the detection probability of the object.**

***Index Terms*—Near-field, optimal aperture, array signal processing, lossy media.**

I. Introduction

In many near-field microwave applications, such as detection and sensing, wireless power transfer to in-body implants, or a data communication link with an implant, two antennas are involved at the receiver and transmitter ends. These antennas are often separated by layers of different lossy media such as skin, fat, muscle tissue, etc. In these applications, high power coupling between the two antennas is desired in order to enhance the detection probability, battery charging efficiency, or increasing the signal-to-noise ratio. That is, to choose the antennas in a way such as to maximize the power coupling between them. The problem can then be modeled by two antenna apertures on opposite sides of a multilayered structure as shown in Fig. 1, where the goal is to synthesize the electric ($\boldsymbol{J}$) and magnetic ($\boldsymbol{M}$) currents on the transmitter aperture such that the ratio of received power on the receiver aperture to the transmitted power is maximized, i.e.,

$$\max_{\boldsymbol{J},\boldsymbol{M}} \left(\frac{P_{\text{out}}}{P_{\text{in}}} \right). \tag{1}$$

Array signal processing techniques have been used previously to determine the optimal distribution of aperture currents that maximizes the near-field power coupling in homogenous lossy media [1], [2]. Therein, the electric and magnetic currents on the transmitter aperture are each expanded in terms of a number of basis functions and the ratio of the received power to the transmitted power can be written in form of a ratio of quadratic forms, the maximum of which can be found with relative ease. This method can be easily expanded to any non-homogenous media as long as the Green's function or the emanated fields from the basis functions are known for the structure.

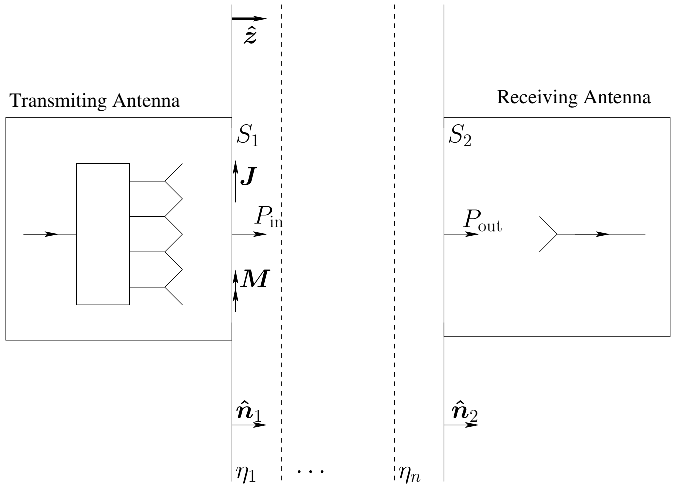

Fig. 1: Power coupling between two apertures separated by a multilayered lossy structure.

Fast and efficient algorithms based on spectral domain methods are available to calculate the Green's functions of multilayered structures [3], where the source current distribution is Fourier-transformed and the spectral domain sources are dealt with in the spatial domain as infinite current sheets. Thereby the multilayered field problem is solved as a problem with known harmonic variations along the transverse dimensions of the structure and the boundary conditions are only applied in the normal direction to the layer boundaries.

By combining these techniques, a numerical method can be developed where the emanated fields from the basis functions can be calculated for arbitrary multilayered structures. These fields are in turn used in the optimization algorithm to determine the optimal aperture current distribution for the given multilayered structure. Furthermore, due to the geometry of the problem, it suffices to calculate the fields for one basis function only, since the fields of the others are identical apart from a spatial translation.

II. Optimization Method

In order to determine the optimal aperture current distribution, the unknown electric ($\boldsymbol{J}$) and magnetic ($\boldsymbol{M}$) currents on the transmitter aperture are each expanded in terms of N basis functions with unknown weights as

$$\boldsymbol{J} = \sum_{n=1}^{N} j_n \boldsymbol{f}_n(\boldsymbol{r}), \quad \text{and} \quad \boldsymbol{M} = \sum_{n=1}^{N} m_n \boldsymbol{g}_n(\boldsymbol{r}). \tag{2}$$

Provided that the emanated field from each basis function at the receiver aperture is known, the power transfer ratio can be written as a ratio of quadratic forms as: (see also [1])

$$P_{\text{tr}} = \frac{P_{\text{out}}}{P_{\text{in}}} = \frac{\mathbf{w}^H \mathbf{P}_{\text{out}} \mathbf{w}}{\mathbf{w}^H \mathbf{P}_{\text{in}} \mathbf{w}} \tag{3}$$

where $\mathbf{P}_{\text{in}}$ and $\mathbf{P}_{\text{out}}$ are Hermitian matrices which define the relation between the input and output powers, respectively, and the transmitter aperture current distribution, and also $\mathbf{w} = [j_1, j_2, \ldots, j_N, m_1, m_2, \ldots, m_N]^T$ is the vector containing the unknown weights of the basis functions in (2). The goal is to determine $\mathbf{w}$ which yields maximum power transfer ratio at a stationary point. This leads to the generalized eigenvalue equation [4]:

$$\mathbf{P}_{\text{out}} \mathbf{w} = P_{\text{tr}} \mathbf{P}_{\text{in}} \mathbf{w}. \tag{4}$$

The maximization of P_{tr} is equivalent to finding the largest eigenvalue in (4) and once $\mathbf{w}$ is determined, the optimal transmitting aperture field distribution can be calculated using (2). It is required that $\mathbf{P}_{\text{in}}$ be a positive definite matrix. This can be ensured by constraining the unknown transmitter currents to Huygen's sources so that the radiated power is positive, i.e.,

$$\boldsymbol{M}(\boldsymbol{r}) = \eta \hat{\boldsymbol{n}}_1 \times \boldsymbol{J} \tag{5}$$

where η is the wave impedance in the medium where the source is located.

III. Green's Function of a Planar Multilayer Structure

G1DMULT is a fast and efficient algorithm for calculating the spectral domain Green's functions of planar, cylindrical and spherical multilayer structures. In the case of the herein employed planar structures, the current sources are in the form of current sheets with harmonic spatial variation [3]. The original 3D current source is transformed to the spectral domain by performing the Fourier transforms

$$\widetilde{\boldsymbol{J}}(k_x, k_y, z) = \int_{-\infty}^{\infty} \int_{-\infty}^{\infty} \boldsymbol{J}(x, y, z) \mathrm{e}^{jk_x x} \mathrm{e}^{jk_y y} \, \mathrm{d}x \, \mathrm{d}y, \tag{6a}$$

$$\widetilde{\boldsymbol{M}}(k_x, k_y, z) = \int_{-\infty}^{\infty} \int_{-\infty}^{\infty} \boldsymbol{M}(x, y, z) \mathrm{e}^{jk_x x} \mathrm{e}^{jk_y y} \, \mathrm{d}x \, \mathrm{d}y. \tag{6b}$$

The sources are interpreted in the spectral domain as a spectrum of current sheets extending to infinity in both the x and y directions, while the problem is divided into an equivalent subproblem for each layer in the structure. Due to the boundary conditions, all the waves have the same propagation constants in x and y directions and the problem is reduced to a harmonic 1D problem in space with known harmonic variations in the x and y directions. The transverse components of the field at the boundaries between the layers are then determined by solving a system of boundary conditions which gives the spectral domain electric $\widetilde{\boldsymbol{E}}(k_x, k_y, z)$ and magnetic $\widetilde{\boldsymbol{H}}(k_x, k_y, z)$ fields. In order to retrieve the 3D fields we need to combine the solutions by a summation over the k_x and k_y spectrum, corresponding to an inverse Fourier transform, i.e.,

$$\boldsymbol{E}(x, y, z) = \frac{1}{4\pi^2} \int_{-\infty}^{\infty} \int_{-\infty}^{\infty} \widetilde{\boldsymbol{E}}(k_x, k_y, z) \mathrm{e}^{-jk_x x} \mathrm{e}^{-jk_y y} \, \mathrm{d}k_x \, \mathrm{d}k_y, \tag{7a}$$

$$\boldsymbol{H}(x, y, z) = \frac{1}{4\pi^2} \int_{-\infty}^{\infty} \int_{-\infty}^{\infty} \widetilde{\boldsymbol{H}}(k_x, k_y, z) \mathrm{e}^{-jk_x x} \mathrm{e}^{-jk_y y} \, \mathrm{d}k_x \, \mathrm{d}k_y. \tag{7b}$$

once the structure and basis functions are defined, it is enough to calculate the emanated fields from a single basis function in order to incorporate G1DMULT in the optimization technique as described in section II. The contributions of the other basis functions can then be found by using a spatial translation corresponding to their location.

IV. Optimization Results

The method is used on a structure consisting of layers of fat ($\epsilon_r = 4.6$, $\sigma = 0.02$ S/m) and muscle tissue ($\epsilon_r = 57$, $\sigma = 1.2$ S/m) at 1 GHz [5]. In the structure, a 4 cm slab of muscle tissue is enclosed by two 1.5 cm layers of fat on two sides. The apertures are hence separated by 7 cm from each other and are assumed to be located in free-space. The transmitter and receiver aperture sizes are assumed to be 5×5 cm^2 and 3×3 cm^2, respectively. Furthermore 2.5×2.5 mm^2 x-polarized rectangular pulse basis function currents are employed as

$$\boldsymbol{f}_n(\boldsymbol{r}) = \hat{\boldsymbol{x}} \Pi(\boldsymbol{r}_n) \quad \text{and} \quad \boldsymbol{g}_n(\boldsymbol{r}) = \hat{\boldsymbol{y}} \Pi(\boldsymbol{r}_n). \tag{8}$$

Due to the presence of loss in the environment, the poles in the integrand in (7) are off the real axis and the integration can be performed along the real axis [6]. The normalized intensities of the electric and magnetic fields radiated by a single basis function located at $\boldsymbol{r}_n = \mathbf{0}$, at the receiver aperture plane, are shown in Fig. 2. Unlike the case of a homogenous material where the field distribution is expected to be similar along the x and y axes, in the case of the multi-layered media the received field distribution is not similar along the two transverse axes. This phenomenon can be explained by the linear polarization of the source current and the different types of incidence (i.e. parallel vs. perpendicular) of the wave at the boundaries in the two directions. The received field due to different basis functions can be calculated separately for each basis function in the spectral domain using the Green's function and then be transformed into the spatial domain, or it can be calculated for one basis function and then for others by using appropriate spatial translation based on the location of

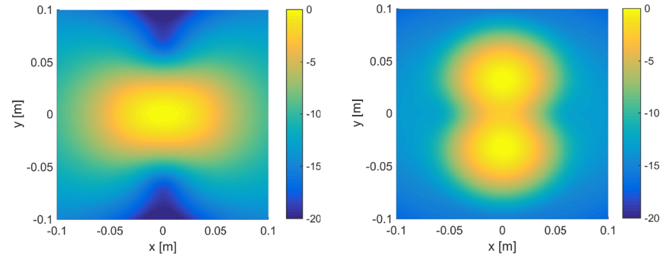

(a) (b)

Fig. 2: Intensity in dB of the (a) electric field, and; (b) magnetic field, radiated by a single basis function at the receiver aperture plane.

that basis function. Here we choose the second approach for simplicity, since it needs only one inverse Fourier transform of the type in (7).

Both the amplitude and phase of the optimal electric current distribution are shown in Fig. 3. As explained in section II, the currents are constrained to Huygen's source distributions in this case. The optimal current distribution exhibits a larger taper rate in the x direction as compared to that in the y direction due to the fact that the field spot from a single basis function is elongated in the x direction. The normal component of the normalized Poynting vector on the receiver aperture, due to the optimal source current, is shown in Fig. 4, which shows that the received power is highest at the center of the receiver aperture and the power decreases towards the edges of the aperture, meaning that the optimal source current results in a focus of power around the center of the receiver aperture.

V. Optimal Aperture in Detection Applications

In detection applications in homogenous media, it has been shown that if the power coupling between two antennas is maximized in the absence of a foreign object, the system sensitivity to the presence of any foreign object is increased [2]. In order to investigate this hypothesis in the case of the multilayered media, we can formulate a method of moments (MoM) approach in the spectral domain to calculate the scattered field from a PEC patch located in the media between the two apertures as shown in Fig. 5. In this figure, z_{t}, z_{p}, and z_{r} are the z coordinates of the transmitter aperture, PEC patch,

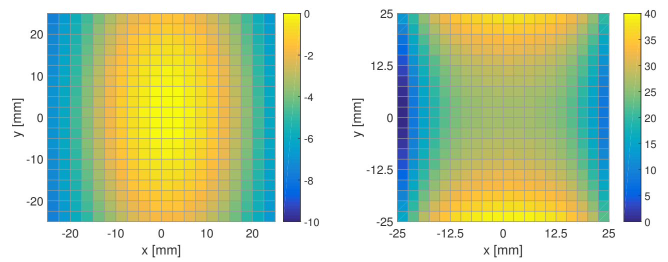

(a) (b)

Fig. 3: (a) Amplitude in dB and, (b) phase in degrees, of the optimized electric current distribution on the transmitter aperture.

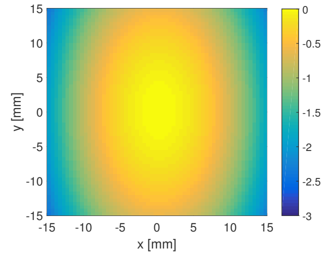

Fig. 4: The normal component of the normalized Poynting vector on the receiver aperture in dB.

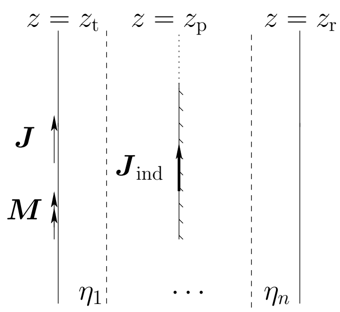

Fig. 5: A PEC patch located in the multilayered media.

and the receiver aperture, respectively.

A. MoM Formulation

Assuming the electric ($\boldsymbol{J}$) and magnetic ($\boldsymbol{M}$) source currents, the induced current ($\boldsymbol{J}_{\mathrm{ind}}$) on the PEC patch can be found by applying the boundary conditions to the tangential electric field on the patch, i.e.

$$\boldsymbol{E}_{\mathrm{tan}}(\boldsymbol{r}) = \boldsymbol{E}^{\mathrm{i}}_{\mathrm{tan}}(\boldsymbol{r}) + \boldsymbol{E}^{\mathrm{s}}_{\mathrm{tan}}(\boldsymbol{r}) = \mathbf{0}, \quad \boldsymbol{r} \in S_{\mathrm{patch}} \tag{9}$$

where $\boldsymbol{E}^{\mathrm{i}}$ and $\boldsymbol{E}^{\mathrm{s}}$ are the incident and the scattered electric fields, respectively. Once the source current is known, the incident field on the patch can be calculated by using the spectral domain Green's function, and expanding the induced current in terms of L basis functions with unknown weights as

$$\boldsymbol{J}_{\mathrm{ind}} = \sum_{n=1}^{L} I_n \boldsymbol{h}_n(\boldsymbol{r}) \tag{10}$$

where $\boldsymbol{h}_n(\boldsymbol{r})$ is the nth basis function and I_n are the unknown weights to be determined. Hence, (9) becomes

$$\boldsymbol{E}^{\mathrm{i}}_{\mathrm{tan}} + \boldsymbol{E}^{\mathrm{s}}_{\mathrm{tan}}(\boldsymbol{J}_{\mathrm{ind}}) = \mathbf{0}, \quad \boldsymbol{r} \in S_{\mathrm{patch}} \tag{11}$$

which, by employing Galerkin's method, becomes:

$$\sum_{n=1}^{L} I_n Z_{mn} = V_m, \quad m = 1, 2, \cdots, L \tag{12}$$

where

$$\begin{aligned} Z_{mn} &= \iint_{\mathrm{patch}} \boldsymbol{h}_m \cdot \boldsymbol{E}^{\mathrm{s}}(\boldsymbol{h}_n)\,\mathrm{d}S, \\ V_m &= -\iint_{\mathrm{patch}} \boldsymbol{h}_m \cdot \boldsymbol{E}^{\mathrm{i}}\,\mathrm{d}S. \end{aligned} \tag{13}$$

In the spectral domain, Z_{mn} can be derived, in a similar manner as in [7], as

$$\begin{aligned}Z_{mn} &= \iint_{\text{patch}} \boldsymbol{h}_m \cdot \boldsymbol{E}^{\mathrm{s}}(\boldsymbol{h}_n)\,\mathrm{d}S \\ &= \frac{1}{4\pi^2}\iint_{k_x,k_y} \widetilde{\boldsymbol{h}}_m(-k_x,-k_y)\cdot \underline{\underline{\widetilde{\mathbf{G}}}}(k_x,k_y,z,z') \\ &\qquad\qquad \cdot \widetilde{\boldsymbol{h}}_n(k_x,k_y)\,\mathrm{d}k_x\,\mathrm{d}k_y\end{aligned} \tag{14}$$

where $z = z' = z_{\mathrm{p}}$, $\widetilde{\boldsymbol{h}}_n(k_x,k_y)$ is the spectral domain representation of $\boldsymbol{h}_n(\boldsymbol{r})$, and $\underline{\underline{\widetilde{\mathbf{G}}}}$ is the spectral domain Green's function. Similarly, V_m is derived as

$$\begin{aligned}V_m &= -\iint_{\text{patch}} \boldsymbol{h}_m \cdot \left[\boldsymbol{E}^{\mathrm{i}}(\boldsymbol{J}) + \boldsymbol{E}^{\mathrm{i}}(\boldsymbol{M})\right]\,\mathrm{d}S \\ &= -\frac{1}{4\pi^2}\iint_{k_x,k_y} \widetilde{\boldsymbol{h}}_m(-k_x,-k_y)\cdot \underline{\underline{\widetilde{\mathbf{G}}}}_J(k_x,k_y,z,z') \\ &\qquad\qquad \cdot \widetilde{\boldsymbol{J}}(k_x,k_y)\,\mathrm{d}k_x\,\mathrm{d}k_y \\ &\quad -\frac{1}{4\pi^2}\iint_{k_x,k_y} \widetilde{\boldsymbol{h}}_m(-k_x,-k_y)\cdot \underline{\underline{\widetilde{\mathbf{G}}}}_M(k_x,k_y,z,z') \\ &\qquad\qquad \cdot \widetilde{\boldsymbol{M}}(k_x,k_y)\,\mathrm{d}k_x\,\mathrm{d}k_y\end{aligned} \tag{15}$$

where $z = z_{\mathrm{t}}$ and $z' = z_{\mathrm{p}}$. Once $\boldsymbol{J}_{\text{ind}}$ is known, the total field on the receiver aperture is found as the sum of the contributions from the source and induced currents.

Since the layers are assumed to be infinitely large, the results of this method can not be generally compared to results of commercial EM simulation softwares such as CST. However, in the special case where all the layers are the same (i.e. homogenous) the two methods can be compared with each other. This has been done for the medium: ϵ_r=1 and σ = 1.2 S/m, where the source has a uniform Huygen's source distribution of size 1×1 m^2, transmitter and receiver apertures are separated by 7 cm, and a 6×6 cm^2 PEC patch is located at 3.5 cm distance from the source. The intensity of the received E-field is shown in Fig. 6 for two orthogonal cuts, which shows very good agreement between the two methods.

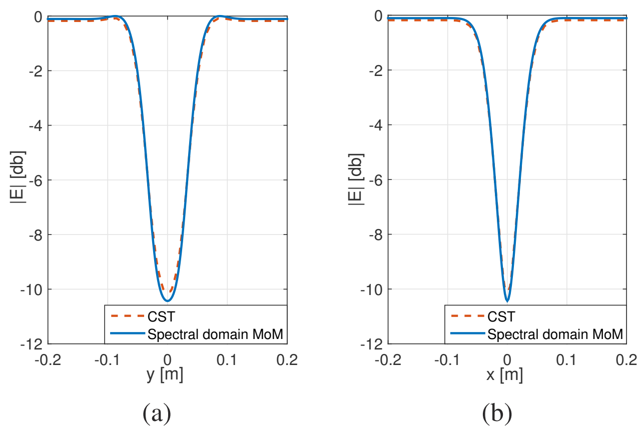

Fig. 6: Comparison of the intensity of the received E-field calculated by CST and the spectral domain MoM in a homogenous medium, in (a) x=0 cut, and; (b) y=0 cut.

B. *Effect of The Source Current Distribution*

The MoM formulation is used to calculate P_{tr} in the presence and absence of a PEC patch for the optimal source current distribution and the subsequent five strongest eigenmodes of (4). These values are then used to calculate the ΔP_{tr} as

$$\Delta P_{\text{tr}} = |P_{\text{tr}}^{\text{PEC}} - P_{\text{tr}}^{\text{free}}| = \frac{|P_{\text{out}}^{\text{PEC}} - P_{\text{out}}^{\text{free}}|}{P_{\text{in}}}. \tag{16}$$

where $P_{\text{tr}}^{\text{PEC}}$ and $P_{\text{tr}}^{\text{free}}$ are the power transfer ratios for each mode in the presence and absence of the PEC patch, respectively, and $P_{\text{in}} = P_{\text{in}}^{\text{PEC}} = P_{\text{in}}^{\text{free}}$ is the input power due to the electric and magnetic current sources. ΔP_{tr} is indicative of the change in measured S_{21} when the two antennas are connected to a network analyzer in a detection system. It is clear that a larger ΔP_{tr} increases the possibility of the detection of a foreign object in the medium. The magnitude of the source currents corresponding to the five largest positive eigenvalues of (4) following the optimal source, are plotted in Fig. 7, for the setup which is introduced in section IV. Assuming that a square PEC patch of side length 1.5 mm is located halfway between the transmitter and receiver apertures (z=3.5 cm) and aligned with the axis connecting the centers of the two apertures, the P_{tr} and ΔP_{tr} of these five modes along with those of the optimal transmitter current (labeled as mode 1) are plotted in Fig. 8. As can be observed in this figure, the optimal transmitter aperture results in the highest ΔP_{tr}, which also occurs at higher P_{tr} value, implying better SNR in a measurement system. Unlike the P_{tr}, which shows a steady decrease with the mode number, the trend in ΔP_{tr} is not monotonous as it is dependent on how much of the power is concentrated at the center of the aperture since the patch is also assumed to be aligned at the center of the two apertures. Any source current distribution can be expanded as a weighted sum of all aperture modes, including those with even lower P_{tr}, hence, the ΔP_{tr} of any other source current distribution is likely to be smaller than that of the optimal aperture.

C. *Effect of The PEC Patch Size*

In any detection system, one figure of merit would be the smallest detectable size of the foreign object. In order to investigate how the choice of aperture field distribution affects this figure, the described MoM formulation is applied to the same problem geometry as in previous subsection, while the size of the PEC patch is varied between 1×1 mm^2 and 30×30 mm^2. Fig. 9 shows the ΔP_{tr} for the choice of the optimal aperture as well as the subsequent five aperture eigenmodes vs. the size of the PEC patch. As expected, the ΔP_{tr} for each eigenmode decreases with a decrease in object size. Furthermore, the optimal aperture field distribution shows the largest change in the P_{tr} value for very small objects among the different distributions, which suggests that the probability of the detection of small objects will be higher using antennas with optimal aperture currents, provided that the power levels are above the system noise floor. Fig. 9 also provides insight in the fundamental limitations of what size of objects one can

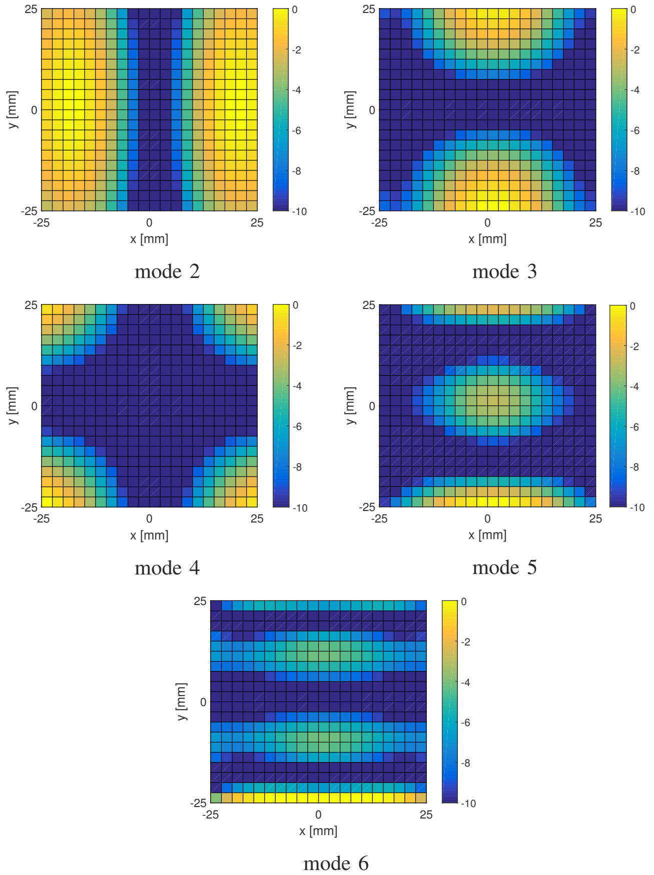

Fig. 7: Magnitude in dB of the source current corresponding to the five largest positive eigenvalues of (4) following the optimal current distribution.

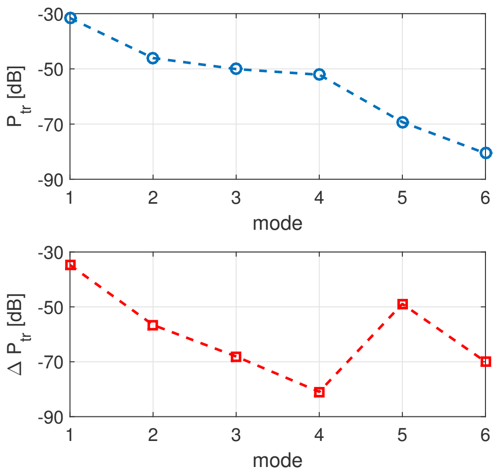

Fig. 8: The P_{tr} (top) and ΔP_{tr} (bottom) of the optimal transmitter current (labeled as mode 1) and the following five modes.

expect to detect, depending on the choice of antennas, system noise level and sensitivity.

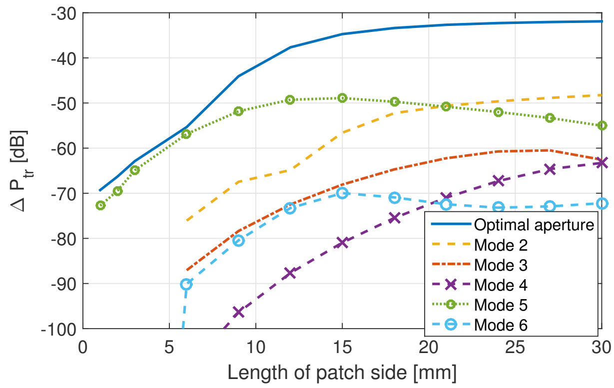

Fig. 9: ΔP_{tr} vs. the size of the PEC patch for the optimal aperture distribution and the following five eigenmodes.

VI. Conclusions

Array-signal-processing and spectral domain techniques are combined in a fast and efficient algorithm, in order to synthesize the optimal aperture current distribution that maximizes the power transfer between two antenna apertures that are located on opposing sides of a multilayered lossy structure in the near-field. The optimal distribution can be used in a range of near-field microwave applications such as sensing and detection, wireless charging of implanted batteries or near-field communications with implants. The Method of Moments is used to calculate the scattered field in the presence of a PEC object in the layered structure in order to investigate the performance of the optimal aperture field distributions in detection applications. The effect of the size of the PEC object is investigated as well, which demonstrates that by employing a suitable antenna aperture, the system sensitivity of detecting foreign objects can be greatly enhanced.

References

[1] A. Razavi, R. Maaskant, J. Yang, and M. Viberg, "Maximum aperture power transmission in lossy homogeneous matters," *Antennas and Wireless Propagation Letters, IEEE*, 2014.

[2] ——, "Optimal aperture distribution for near-field detection of foreign objects in lossy media." Palm beach, Aruba: IEEE-APS Topical Conference on Antennas and Propagation in Wireless Communications, (IEEE APWC '14), August 2014.

[3] Z. Šipuš, P.-S. Kildal, R. Leijon, and M. Johansson, "An algorithm for calculating Green's functions of planar, circular cylindrical, and spherical multilayer substrates," *Applied Computational Electromagnetics Society (ACES) Journal*, no. 3, pp. 243–254, 1998.

[4] R. F. Harrington, *Field Computation by Moment Methods*. New York: The Macmillan Company, 1968.

[5] S. Gabriel, R. Lau, and C. Gabriel, "The dielectric properties of biological tissues: III. Parametric models for the dielectric spectrum of tissues," *Physics in medicine and biology*, vol. 41, p. 2271, 1996.

[6] N. K. Uzunoglu, N. G. Alexopoulos, and J. G. Fikioris, "Radiation properties of microstrip dipoles," *IEEE Transactions on Antennas and Propagation*, vol. 27, no. 6, pp. 853–858, November 1979.

[7] D. M. Pozar, "Input impedance and mutual coupling of rectangular microstrip antennas," *IEEE Transactions on Antennas and Propagation*, vol. 30, no. 6, pp. 1191–1196, November 1982.